



HAL
open science

Heat flow, morphology, pore fluids and hydrothermal circulation in a typical Mid-Atlantic Ridge flank near Oceanographer Fracture Zone

V. Le Gal, F. Lucazeau, M. Cannat, J. Poort, C. Monnin, A. Battani, F. Fontaine, B. Goutorbe, F. Rolandone, Christine Poitou, et al.

► **To cite this version:**

V. Le Gal, F. Lucazeau, M. Cannat, J. Poort, C. Monnin, et al.. Heat flow, morphology, pore fluids and hydrothermal circulation in a typical Mid-Atlantic Ridge flank near Oceanographer Fracture Zone. *Earth and Planetary Science Letters*, 2018, 482, pp.423 - 433. 10.1016/j.epsl.2017.11.035 . hal-01793115

HAL Id: hal-01793115

<https://ifp.hal.science/hal-01793115>

Submitted on 29 Jan 2019

HAL is a multi-disciplinary open access archive for the deposit and dissemination of scientific research documents, whether they are published or not. The documents may come from teaching and research institutions in France or abroad, or from public or private research centers.

L'archive ouverte pluridisciplinaire **HAL**, est destinée au dépôt et à la diffusion de documents scientifiques de niveau recherche, publiés ou non, émanant des établissements d'enseignement et de recherche français ou étrangers, des laboratoires publics ou privés.



Distributed under a Creative Commons Attribution - NonCommercial - NoDerivatives 4.0 International License



Heat flow, morphology, pore fluids and hydrothermal circulation in a typical Mid-Atlantic Ridge flank near Oceanographer Fracture Zone

V. Le Gal^{b,d,*}, F. Lucazeau^a, M. Cannat^a, J. Poort^b, C. Monnin^c, A. Battani^d, F. Fontaine^a, B. Goutorbe^e, F. Rolandone^b, C. Poitou^a, M.-M. Blanc-Valleron^f, A. Piedade^g, A. Hipólito^h

^a Institut de Physique du Globe de Paris/Sorbonne Paris Cité, UMR CNRS 7154, 1 rue Jussieu, 75238, Paris cedex 05, France

^b iSTeP, Université Pierre et Marie Curie, 4 place Jussieu, 75252, Paris cedex 05, France

^c Geosciences Environnement Toulouse, 14 Avenue Edouard Belin, 31400, Toulouse, France

^d Geosciences, IFP Energies nouvelles, 1-4 avenue de Bois-Préau, 92852 Rueil-Malmaison Cedex, France

^e Universidade Federal Fluminense, Niterói, Brazil

^f Muséum National d'Histoire Naturelle, CP 48, 57 rue Cuvier, 75231 Paris cedex 05, France

^g School of Earth and Ocean Sciences, Cardiff University, Main Building, Park Place, CF10 3AT Cardiff, United Kingdom

^h Universidade dos Açores, Departamento de Geociências, Rua da Mãe de Deus, 9501-801 Ponta Delgada, Portugal

ARTICLE INFO

Article history:

Received 6 June 2017

Received in revised form 9 November 2017

Accepted 14 November 2017

Available online 24 November 2017

Editor: M. Bickle

Keywords:

heat flow

pore water

Oceanographer Fracture Zone

hydrothermal circulation

Mid-Atlantic Ridge flank

morphology

ABSTRACT

Hydrothermal circulation affects heat and mass transfers in the oceanic lithosphere, not only at the ridge axis but also on their flanks, where the magnitude of this process has been related to sediment blanket and seamounts density. This was documented in several areas of the Pacific Ocean by heat flow measurements and pore water analysis. However, as the morphology of Atlantic and Indian ridge flanks is generally rougher than in the Pacific, these regions of slow and ultra-slow accretion may be affected by hydrothermal processes of different regimes. We carried out a survey of two regions on the eastern and western flanks of the Mid-Atlantic Ridge between Oceanographer and Hayes fracture zones. Two hundred and eight new heat flow measurements were obtained along six seismic profiles, on 5 to 14 Ma old seafloor. Thirty sediment cores (from which porewaters have been extracted) have been collected with a Kullenberg corer equipped with thermistors thus allowing simultaneous heat flow measurement. Most heat flow values are lower than those predicted by purely conductive cooling models, with some local variations and exceptions: heat flow values on the eastern flank of the study area are more variable than on the western flank, where they tend to increase westward as the sedimentary cover in the basins becomes thicker and more continuous. Heat flow is also higher, on average, on the northern sides of both the western and eastern field regions and includes values close to conductive predictions near the Oceanographer Fracture Zone. All the sediment porewaters have a chemical composition similar to that of bottom seawater (no anomaly linked to fluid circulation has been detected). Heat flow values and pore fluid compositions are consistent with fluid circulation in volcanic rocks below the sediment. The short distances between seamounts and short fluid pathways explain that fluids flowing in the basaltic aquifer below the sediment have remained cool and unaltered. Finally, relief at small-scale is calculated using variogram of bathymetry and compared for different regions affected by hydrothermal circulation.

© 2017 The Authors. Published by Elsevier B.V. This is an open access article under the CC BY-NC-ND license (<http://creativecommons.org/licenses/by-nc-nd/4.0/>).

1. Introduction

Oceanic heat flow is commonly affected by perturbations attributed to hydrothermal circulation (Lister, 1972). Although near-axis processes have more spectacular manifestations (black or white smokers), ridge-flank hydrothermal circulation also contributes to significant advective heat loss (Stein and Stein, 1992, 1994) and chemical fluxes (Fisher and Wheat, 2010) to the oceans.

Because hydrothermal circulation affects mainly the uppermost part of the lithosphere, it has little effect on its subsidence. Therefore, conductive models (e.g. Sclater and Francheteau, 1970; Davis and Lister, 1974) are often used to define a theoretical heat flow value for a specific age of the sea-floor: Stein and Stein (1992) have shown, for instance, that heat flow measurements are statistically lower than theoretical values for ages younger than 60 Ma.

Low seafloor heat flow on young ridge flanks is commonly interpreted as a consequence of shallow hydrothermal circulation in the upper basaltic basement, which is much more permeable than the sediments. This process has been understood from observa-

* Corresponding author.

E-mail address: legal.vg@gmail.com (V. Le Gal).

tions of regional studies (e.g. Davis et al., 1989, 1992, 1997; Fisher et al., 2003a; Wheat et al., 2004): in the eastern Juan de Fuca area where oceanic basement is covered by a thick sediment blanket (~400 m), fluids can recharge or discharge at seamounts, and they can flow in the uppermost basalts over distance of several tens of kilometers (Fisher et al., 2003a). Surface heat flow is perturbed significantly near recharge and discharge areas, but is more or less close to the theoretical value at some distance from the seamounts: a simple well-mixed aquifer model (Langseth and Herman, 1981) gives estimates of this distance as a function of fluid velocity and aquifer thickness. On the eastern flank of the Juan de Fuca Ridge, this critical distance varies from 2–5 km in the Second Ridge area (3.5 M.y. seafloor) to about 20 km in the Hydrothermal Transition area (1.1–1.3 M.y. seafloor) (Hutnak et al., 2006). In other locations where sediment is thinner and less continuous, cold fluids mining surface heat flow might dominate because they have not had time to equilibrate with the host rock (Fisher et al., 2003b; Hutnak et al., 2008). Indeed, the statistical differences observed with conductive values for ages less than 60 Ma (Stein and Stein, 1992) suggest that most of oceanic heat flow data gathered in the global database are more affected by hydrothermal circulation than in the Second Ridge area of the eastern Juan de Fuca Ridge flank.

Heat flow in the mid-Atlantic (Langseth et al., 1966) or Indian (e.g. Crozet and Madagascar basin, Anderson et al., 1979) ridge flanks is statistically lower for the same age than heat flow in the Pacific. An exception was observed by Lucazeau et al. (2006) near the Lucky-Strike segment of the Mid-Atlantic-Ridge (MAR), where the sediment thickness is relatively continuous and the heat flow reaches conductive values in the same way as in the Hydrothermal Transition of the eastern Juan de Fuca Ridge flank. Where the morphology is rougher and the sedimentation in basins less continuous as in most of the Atlantic or Indian oceans, hydrothermal cooling appears much more important. For instance, data in the Atlantic site known as “North Pond” (Langseth et al., 1992; Schmidt-Schierhorn et al., 2012) shows that surface heat flow is uniformly low compared to the conductive values, which attests of a large scale depletion of heat, but increases from east to west (~4 km from one flank of the pond to the other one).

Hydrothermal circulation also modifies the composition of fluids and rocks, through alteration or diagenetic processes. These changes in fluid composition can be detected by measuring the chemical concentration gradients in the sedimentary column. A typical reaction results from the alteration of basaltic glass into palagonite, smectite and then carbonate (Staudigel et al., 1981). Magnesium is removed from basalt and replaced by calcium extracted from seawater, which is conversely enriched in magnesium (Seyfried and Mottl, 1982). Therefore, fluids flowing within the basement can be progressively modified compared to seawater if reactions are rapid and/or residence time is sufficiently long, resulting in a gradient of concentration between bottom seawater and the basaltic aquifer. The amount of calcium and magnesium exchanged during these reactions depends on temperature and time, and Fisher and Wheat (2010) show that large flow rates and short residence times would result in smaller composition changes of the fluids. Near discharge areas, upward fluid flow in sediments may be detected, because this flow disturbs the linearity of otherwise diffusive Ca^{2+} and Mg^{2+} concentration gradients in the uppermost meters. Therefore, pore fluid geochemistry is a useful and complementary tool in oceanic heat flow measurements in order to understand hydrothermal systems.

This study presents new results of a marine survey on the flanks of the Mid-Atlantic ridge (MAR). This is the first systematic approach on a slow spreading ridge area with such a large number of heat flow data (208 measurements). The goal was to combine heat flow and pore fluid measurements that could com-

pare, in term of scale and size, to the Juan de Fuca area but with a typical morphology of the Atlantic.

2. Geological context

The survey was carried out in the northern part of the Oceanographer-Hayes segment (OH1), where a previous geophysical study (SudAçores) was already available (Cannat et al., 1999; Rabain et al., 2001). The study area is adjacent to the first segment of the MAR south of the Oceanographer Fracture Zone (OFZ), a major right-lateral offset at approximately 35°N and 35–36°W, about 500 km of the Azores islands (Fig. 1). The MAR south of the OFZ is divided into four second-order segments OH1 to OH4 (Detrick et al., 1995), which are separated by broad left-lateral non transform offsets. The present study focuses on 5 to 14 Ma crust ages in the OH1 area. A pronounced mantle Bouguer gravity low is associated with the central part of OH1, attesting a thicker crust (8–8.5 km) compared to that at the end (3.5–5.0 km) of the segment (Rabain et al., 2001; Dunn et al., 2005). Oceanic accretion is accommodated by magmatism in the central part and by tectonic processes at the segment ends. The SudAçores survey acquired multibeam bathymetry, gravity and magnetic data that defines the structural evolution of OH1 (Rabain et al., 2001). A prominent seamount chain spreads on both flanks from the present axis to a seafloor age of ~6 Ma. This chain is interpreted as a consequence of the focused magmatism, which also contributed to the acceleration of a southward propagation of this segment (Rabain et al., 2001). In the domain where this chain of seamounts is observed, there was not enough sediment to measure surface heat flow, but the morphology resulting from the enhanced volcanic activity should significantly contribute to the hydrothermal system. Sedimentary deposits are mainly detrital carbonates with foraminifer nanofossils (Bougault et al., 1985). The sediment thickness in the field area of the present study, based on the SudAçores seismic profiles, is 0 to 300 m.

3. Methodology

The Oceanograflu survey was carried out in May–June 2013 on R/V “l’Atalante”. It was entirely devoted to the study of heat and fluid transfer on both ridge flanks south of the OFZ, and combined heat flow measurements and sampling of pore fluids for geochemistry. All measurements from this study were acquired along seismic and CHIRP profiles from the SudAçores geophysical survey (Cannat et al., 1999).

3.1. Heat flow

Oceanic heat flow, which represents the conductive heat loss rate per unit surface area of the Earth, can be determined as the product of the vertical temperature gradient and thermal conductivity. On ridge flanks, seafloor heat flow can be significantly perturbed by the redistribution of heat by fluid circulation. This allows heat flow data to be used to constrain the geometry and magnitude of perturbations caused by hydrothermal circulation in the underlying rocks. Two measurement techniques were used during Oceanograflu: conventional multi-penetration measurements and Küllenberg (piston) cores equipped with NKE@autonomous thermal probes mounted on outriggers. Both techniques give a temperature resolution of better than 5/1000 K. The multi-penetration instrument is derived from the Von Herzen’s outrigger instrument (Von Herzen et al., 1989): it includes a five meter long barrel equipped with seven outrigger thermistors, and a 1.5 ton weight ensuring penetration into soft sediment. Data acquisition is real-time controlled by an acoustic system of communication, and the acquisition sequence is also recorded on a compact-flash

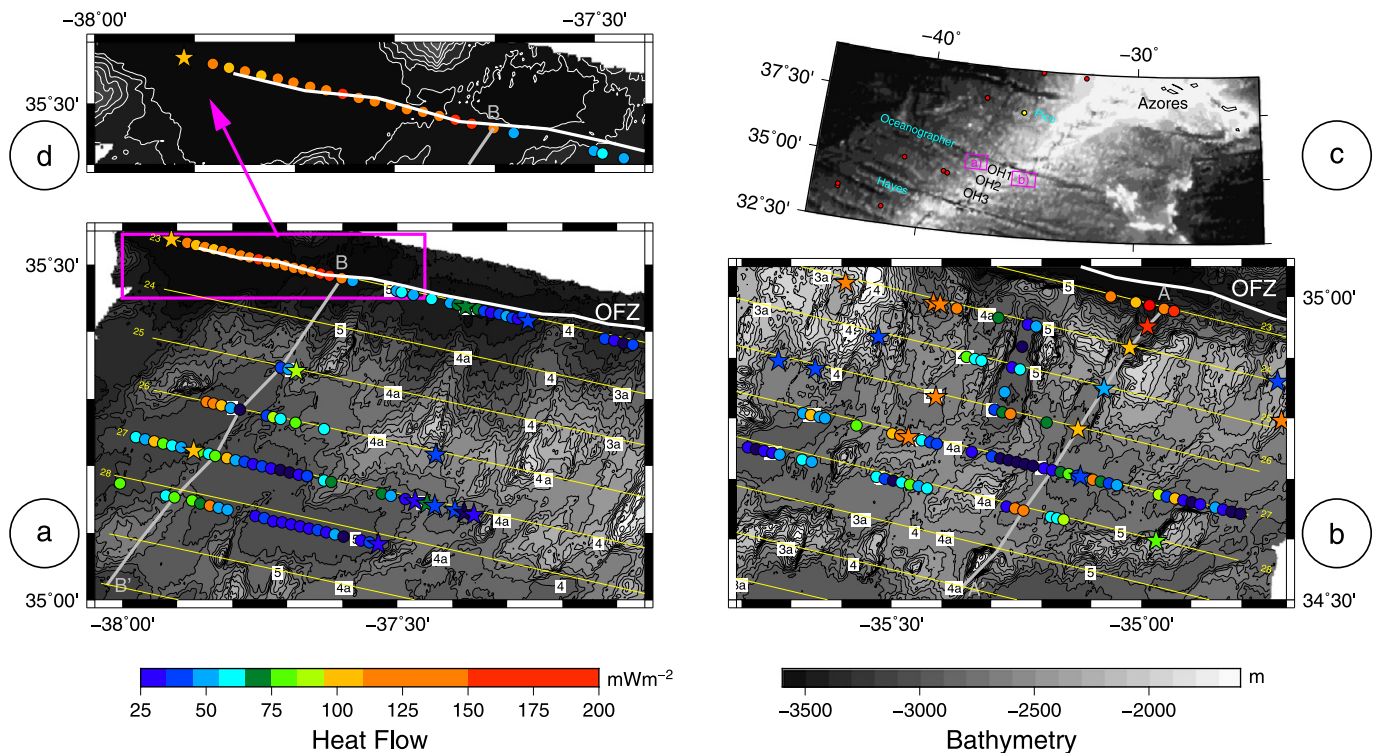


Fig. 1. Distribution and magnitude of heat flow on bathymetric maps: a) heat flow measurements on the western flank; b) heat flow measurements on the eastern flank; c) location of the study areas, Azores islands, holes from DSDP 82 (red circles) and DSDP 94 (yellow circle), and the three major fracture zones: Pico, Oceanographer and Hayes. Background corresponds to multibeam bathymetry (Gtopo30 for the inset); d) close up view of heat flow measurements near the Oceanographer Fracture Zone. Heat flow values are reported as circles for multi penetration probes and stars for measurements associated with Küllenberg cores; colors refer to the heat flow scale. The white line represents the morphological trace of OFZ and the yellow lines represent seismic profiles. Isochrons identified during the SudAçores survey (Rabain et al., 2001) are represented by a white box with the anomaly number: anomaly 3 \simeq 4.18 Ma, anomaly 3a \simeq 5.89 Ma, anomaly 4 \simeq 7.43 Ma, anomaly 4a \simeq 8.69 Ma and anomaly 5 \simeq 9.74 Ma. Profiles AA' and BB' are reconstructed profiles shown in supplementary material. Bathymetry scale is the same for a, b and d, with 100 m isolines equidistance. (For interpretation of the colors in this figure, the reader is referred to the web version of this article.)

card in the instrument. The acquisition sequence includes a record of (i) the temperature decrease after a peak caused by frictional heating when the instrument penetrates into the sediment and (ii) the temperature increase caused by a continuous and controlled heating of the thermistors. The first part of the sequence allows extrapolation of the equilibrium temperature, while the second part is used to determine in-situ thermal conductivity. Using this system, a series of several heat flow measurements can be done without pulling up the instrument on the deck, saving time which increases the spatial resolution of the measurements: a typical “station” acquires 15 to 30 heat flow measurements over 24 to 48 h. 178 multi-penetration heat flow measurements obtained during 12 stations and 30 other measurements from Küllenberg cores were obtained (Table 2 in Supplementary Material provides the location and characteristics for all measurements). All of them have been corrected for tilt, sedimentation, topography and heat refraction at the basement–sediment interface.

The two types of instruments provide consistent results from duplicate measurements (e.g. OCN2-1 vs KT1 or OCN2-10 vs KT2) or trends observed along a profile where both instruments were used. In situ thermal conductivities are statistically 5 percent higher than laboratory measurements (0.96 and 0.90 W/m/K respectively). More information on the methods and corrections can be found in the Supplementary Material.

3.2. Pore water geochemistry

Cores were collected at thirty locations during the Oceanograflu survey, returning 0.8 to 4.80 m of sediment. All cores were cut into 1.5 m long sections and sent to a cold laboratory (8 °C) for fluid extraction. Sampling was performed every 10 cm in the upper

first meter (in order to detect curvature of concentration gradients), and then every 40 cm below 1 m. A standard procedure (Seeborg-Elverfeldt et al., 2005) was applied to extract pore waters with rhyzons©. Pore waters have been analyzed for all major and minor elements (Ca^{2+} , Mg^{2+} , Na^+ , K^+ , Sr^{2+} , Mn^{2+} , Li^+ , Ba^{2+} , $\text{B}(\text{OH})_3$) in fourteen cores. More details on the procedure and analytical techniques can be found in the Supplementary Material.

4. Results

4.1. Heat flow measurements

The distribution and average values of heat flow on the western and eastern flanks, respectively $65.9 \pm 38.3 \text{ mWm}^{-2}$ and $67.7 \pm 44.0 \text{ mWm}^{-2}$, are not statistically different (see histogram of values in supplementary material). This represents 40 percent of the theoretical conductive value for this age of the crust, in agreement with global analysis (e.g. Stein and Stein, 1992). However, the magnitude of the heat flow (HF) or corrected heat flow (CTHF) and its analytical error (σ_{HF}) vary significantly from place to place.

We divide the measurements into two main categories characterized by: (i) a limited penetration of the instrument, a non linear thermal gradient and usually low heat flow values and (ii) a full penetration, a more linear gradient and higher heat flow. Why penetration was difficult and the temperature gradient at some locations is not as linear as for other measurements is not clear without further investigation: where we recovered cores, their structure and composition were not that significantly different, and the sub-bottom profiler did not show any special reflection that could attest of a harder bottom.

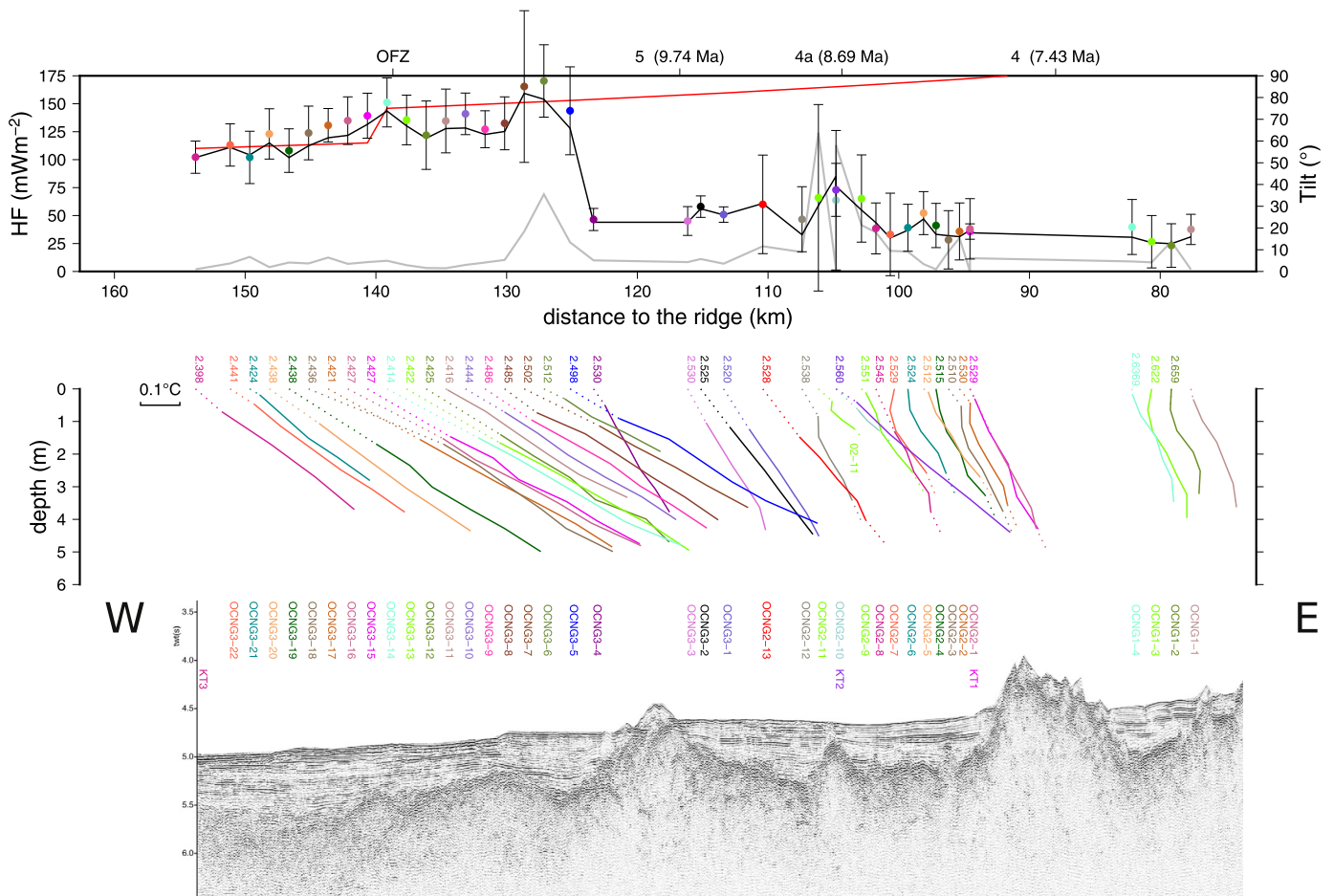


Fig. 2. Heat flow measurements along seismic profile 23W. Upper panel shows heat flow (dots, black line) and tilt (grey line). Black line represents raw heat flow values, while dots represent heat flow corrected for sedimentation, topography and heat refraction, with the associated error (3σ or 99.7% confidence interval). Red line represents the conductive heat flow based on Stein and Stein (1992) model (note the step on the western part). Top of the panel shows isochrons and OFZ locations. Bottom of the panel is the distance to the ridge axis. Middle panel represents temperature versus depth profiles with arbitrary temperature scale. Surface temperature is indicated at the top of each profile. Dotted lines represent extrapolations. Bottom panel represents the seismic profile at the same horizontal scale and position of each site (multi penetration or core) above. The vertical scale is Two Way Travel time (s). (For interpretation of the references to color in this figure, the reader is referred to the web version of this article.)

The distribution of heat flow in map view (Fig. 1) shows some noticeable characteristics: (i) values on the eastern flank of the ridge are more erratic than values on the western flank and on the vicinity of OFZ, (ii) heat flow increases significantly with age of the sea-floor on the western flank and (iii) an abrupt transition of heat flow values toward high values is observed in the northwestern part of the study. The distribution of temperature gradients and heat flow along profiles shows further characteristics. Profile 23W, located in the northwestern part of the study, shows an abrupt transition (over 2 km, Fig. 2) between low heat flow values on the eastern part of the profile and near conductive values on the older western part of the profile. A similar thermal transition was observed previously on the Coco plate (Fisher et al., 2003b) and attributed to the presence of a shallow hydrothermal circulation (Hutnak et al., 2007). The transition occurs at a distance of about 5 km from a seamount, but the closest measurement (OCNG3-4) on its western side remains as low as measurements on its eastern side (Fig. 2). An other characteristic of this profile is the occurrence of a buried basement high above which heat flow measurements have been obtained with both OCNG2-10 and Küllenberg core KT2: heat flow is slightly higher ($\sim 70 \text{ mWm}^{-2}$) but not as much as above basement highs on 3.5 Ma old seafloor on the east flank of Juan de Fuca Ridge (Davis et al., 1997; Hutnak et al., 2006). The temperature vs depth profiles also tends to be much more linear

in the west where heat flow is higher. On the eastern ridge flank along the same seismic profile (23E), the basement morphology is more rugose and sediment is thinner and patchier, with several basement highs and only few and narrow basins (Fig. 3), allowing only five measurements. However, all of these have high values around the predicted conductive heat flow average, and display linear gradients.

In the central part of the OH1 segment, the thermal regime is apparently more affected by hydrothermal circulation. On the western ridge flank (Figs. 1 and 4), although heat flow progressively increases westward as the size of basins increases, we do not observe a clear zone of conductive heat flow as near the OFZ. On the eastern ridge flank (Figs. 1 and 5), there are more basement outcrops and sediment cover is less continuous. The surface of the sediment is also more chaotic and affected by small post-deposition displacements. In this region, heat flow is systematically low, temperature vs depth profiles are not linear and the instruments rarely penetrated completely into the sediment (Fig. 5). The lowest heat flow values of this profile (OCNG 8-12 to 8-17) were measured in a perched basin, but it is generally difficult to define a clear organization of values. This chaotic pattern is also observed on other profiles in the eastern ridge flank (profiles 25E, 26E, 28E, provided in the Supplementary Material).

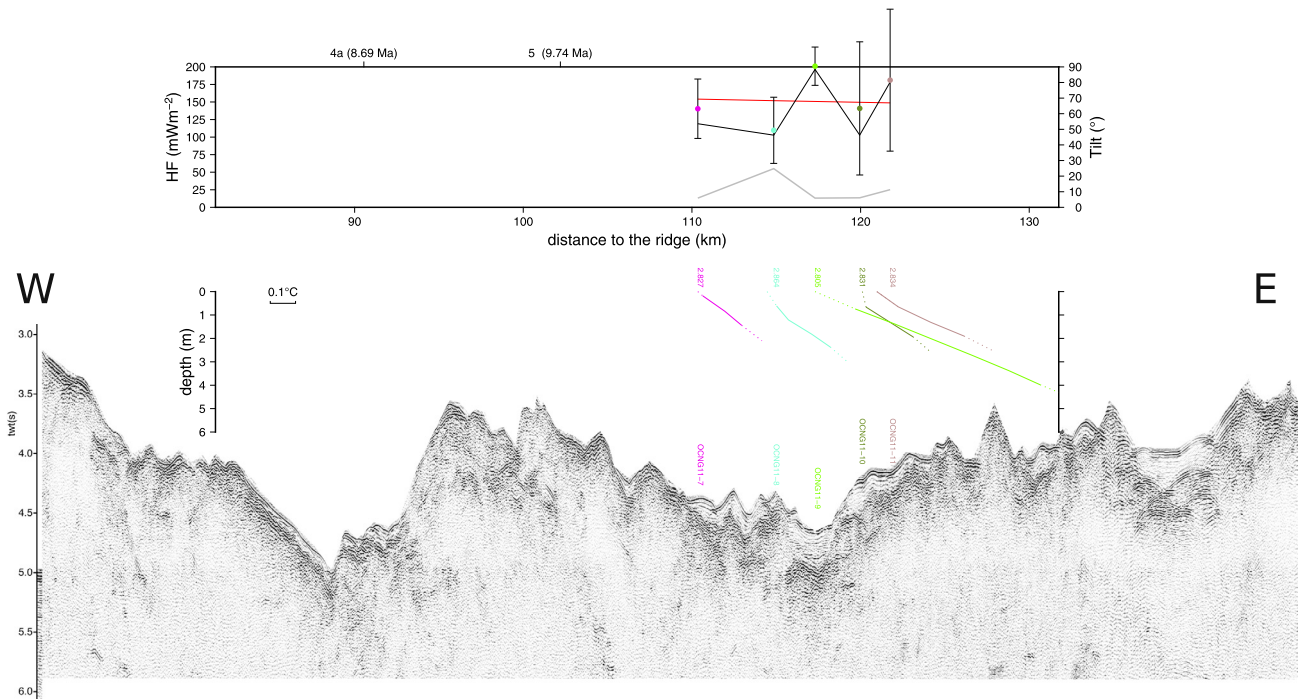


Fig. 3. Heat flow measurements along seismic profile 23E. Upper panel shows heat flow (dots, black line) and tilt (grey line). Black line represents raw heat flow values, while dots represent heat flow corrected for sedimentation, topography and heat refraction, with the associated error (3σ or 99.7% confidence interval). Red line represents the conductive heat flow based on Stein and Stein (1992) model. Top of the panel shows isochrons locations. Bottom of the panel is the distance to the ridge axis. Middle panel represents temperature versus depth profiles with arbitrary temperature scale. Surface temperature is indicated at the top of each profile. Dotted lines represent extrapolations. Bottom panel represents the seismic profile at the same horizontal scale and position of each site (multi penetration or core) above. The vertical scale is Two Way Travel time (s). (For interpretation of the references to color in this figure, the reader is referred to the web version of this article.)

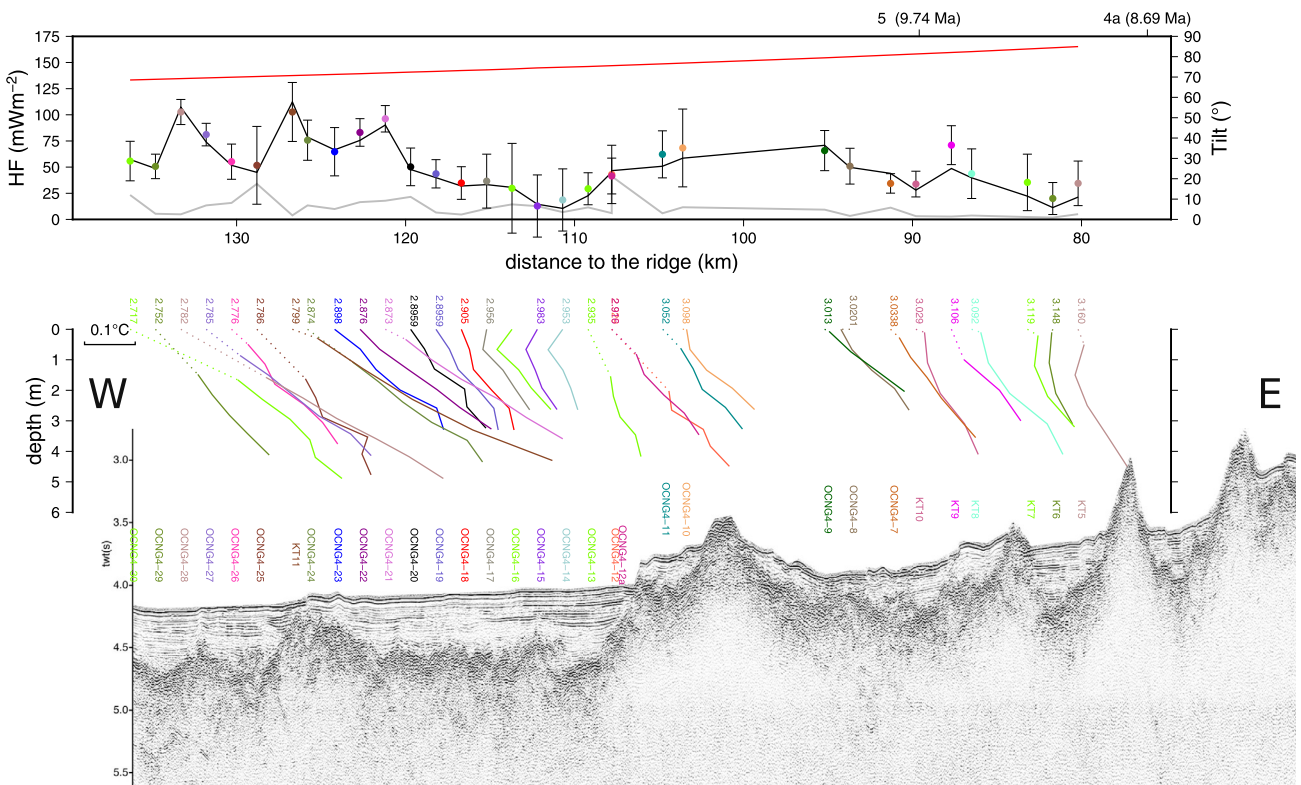


Fig. 4. Heat flow measurements along seismic profile 27W. Upper panel shows heat flow (dots, black line) and tilt (grey line). Black line represents raw heat flow values, while dots represent heat flow corrected for sedimentation, topography and heat refraction, with the associated error (3σ or 99.7% confidence interval). Red line represents the conductive heat flow based on Stein and Stein (1992) model. Top of the panel shows isochrons locations. Bottom of the panel is the distance to the ridge axis. Middle panel represents temperature versus depth profiles with arbitrary temperature scale. Surface temperature is indicated at the top of each profile. Dotted lines represent extrapolations. Bottom panel represents the seismic profile at the same horizontal scale and position of each site (multi penetration or core) above. The vertical scale is Two Way Travel time (s). (For interpretation of the references to color in this figure, the reader is referred to the web version of this article.)

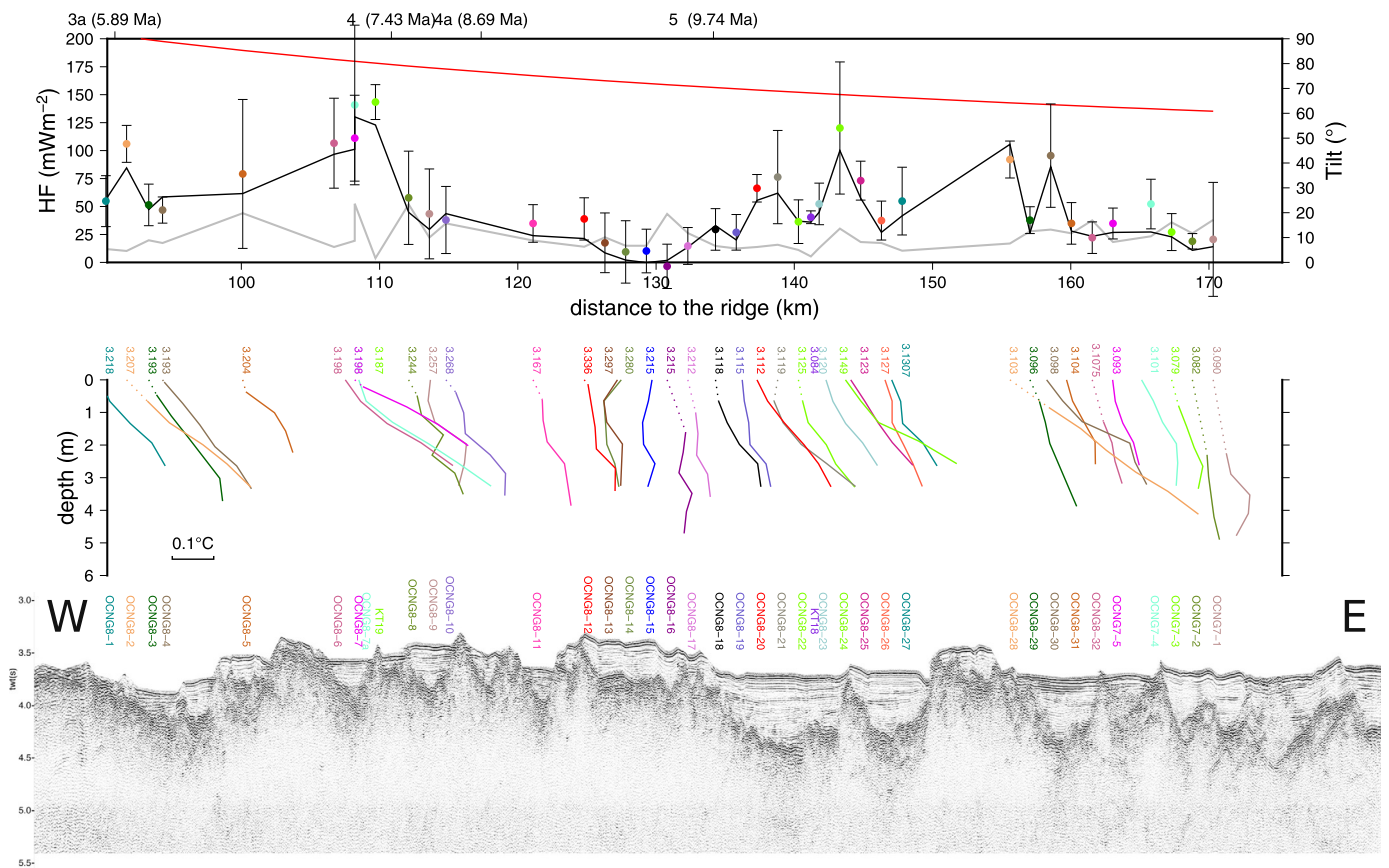


Fig. 5. Heat flow measurements along seismic profile 27E. Upper panel shows heat flow (dots, black line) and tilt (grey line). Black line represents raw heat flow values, while dots represent heat flow corrected for sedimentation, topography and heat refraction, with the associated error (3σ or 99.7% confidence interval). Red line represents the conductive heat flow based on [Stein and Stein \(1992\)](#) model. Top of the panel shows isochrons locations. Bottom of the panel is the distance to the ridge axis. Middle panel represents temperature versus depth profiles with arbitrary temperature scale. Surface temperature is indicated at the top of each profile. Dotted lines represent extrapolations. Bottom panel represents the seismic profile at the same horizontal scale and position of each site (multi penetration or core) above. The vertical scale is Two Way Travel time (s). (For interpretation of the references to color in this figure, the reader is referred to the web version of this article.)

4.2. Pore water geochemistry

The abundance of major cations and anions (Na^+ , Ca^{2+} , K^+ , Mg^{2+} , Cl^- , SO_4^{2-}) and minor ions (Sr^{2+} , $\text{B}(\text{OH})_3$, Ba^+ , Mn^{2+} , Li^+) has been systematically determined in pore waters. All concentrations are close to seawater values ([Millero et al., 2006](#)), with the exception of small variations for manganese. For example, calcium concentrations range from 10 to 11.5 mmol/kg (seawater 10.3 mmol/kg), magnesium from 53 to 57 mmol/kg (seawater 53 mmol/kg), chloride from 550 to 580 mmol/kg (seawater 546 mmol/kg) and sulfates from 27 to 29.5 mmol/kg (seawater 28 mmol/kg). Manganese concentration reaches a maximum of 60 $\mu\text{mol/kg}$ in 8 cores whereas seawater concentration is basically 0. This non zero concentration is probably caused by early diagenetic reactions during oxidation of organic matter ([Berner, 1971](#)). More details on the geochemical results can be found in the Supplementary Material. In this paper, we focus our discussion on the calcium and magnesium concentrations, because they are typical tracers of fluid interactions with the basaltic upper crust.

4.3. Basement morphology

Previous studies have shown the important role of basement morphology in the development of hydrothermal systems, especially the density of seamounts and the distance between them.

In the present study, heat flow is obviously influenced by basement morphology, but it is difficult to relate the observed heat flow patterns to a simple hydrothermal system where fluids enter at one identified seamount and discharge at another ([Langseth and Herman, 1981](#); [Hutnak et al., 2006](#)). This may be because multiple outcrops help to guide recharge and discharge, including outcrops that are oriented out of the plane of individual seismic profiles. Flow may also be guided, at least in part, by ridge-parallel faults and fractures. Without seismic lines in other directions, seafloor morphology can be used to characterize the ridge flank roughness. Variograms of the topography, which represents the statistical difference between two points as a function of their distance, provide a simple way to characterize relief at various spatial scales and for various directions ([Mathéron and Krumbein, 1970](#)). Variograms are generally characterized by three important parameters ([Fig. 6](#) and [Roko et al., 1997](#)), (i) the *nugget* which characterizes here the local relief, (ii) the *sill* which represents the limit when relief stabilizes and (iii) the *lag* which is the correlation length (or distance to the sill). Variograms are calculated for the western and eastern flank area of OH1 ([Fig. 6](#)): lag is smaller for the eastern flank, but sills are similar (400 m). Relief in the spreading direction is also less than relief along a direction perpendicular to spreading ([Fig. 6](#)), about 2 and 1.5 times more on the western and eastern flank respectively.

5. Discussion

Most heat flow measurements on the flanks of the Mid-Atlantic Ridge in the OH1 segment are low (Figs. 2–5) compared to the predicted values from conductive cooling models (e.g. Stein and Stein, 1992). Some measurements approach these conductive values, mostly in the western and northern part of the study. In addition, several of the measured temperature versus depth profiles are not linear, showing curvatures or sigmoid shapes. Finally, all pore fluid analyses record essentially the same composition as seawater.

5.1. Conductive versus low heat flow in the OH1 segment of the Mid-Atlantic Ridge

Almost all near conductive values are observed along profile 23 (Figs. 2–3). It is therefore interesting to question why these values are located here, especially as they are observed on both flanks where the morphology is quite different. Profile 23 is the closest to the OFZ (Fig. 1). On the eastern ridge flank, heat flow measurements are located in front of the North segment ridge. However, average heat flow ($155 \pm 33 \text{ mW m}^{-2}$) corresponds to the conductive values expected for this 11 Ma-old crust (154 mW m^{-2} according to Stein and Stein, 1992). On the western ridge flank, profile 23 follows and then crosses over the trace of OFZ at its western end: the age of the sea-floor in the North segment is older ($\approx 20 \text{ Ma}$) than the age documented in OH1 (11 Ma, Rabain et al., 2001). Heat flow values decrease accordingly to $110 \pm 10 \text{ mW m}^{-2}$ in the North segment, in agreement also with conductive values predicted for 20 Ma age of the seafloor (Stein and Stein, 1992). In addition to the observations of conductive values along profile 23, the transition from low heat flow at 125 km (Fig. 2) is remarkably abrupt: if fluid flowed horizontally below the sediment to the west in the direction of the profile, the well-mixed aquifer model (Langseth and Herman, 1981) would predict a more progressive transition for similar conditions. Instead, this pattern looks very similar to those on the Cocos Plate at the thermal transitions between warmer and cooler parts (Fisher et al., 2003b; Hutnak and Fisher, 2007). Low heat flow is maintained to the east on profile 23, where many basement outcrops exist, some of which could be sites of hydrothermal discharge.

The heat flow trend along profile 27W (Fig. 4) does not reach conductive cooling values, but is similar to that of profile 23W: heat flow values are low on the eastern part of the profile, closer to the ridge, and higher in the west, where the sedimentary basins become more continuous. Temperature versus depth profiles also tend to be more linear in the western part of profile 27W. In profile 27E (Fig. 5), heat flow is low or very low, and does not increase with seafloor age as observed in profile 27W. The lowest values are observed where the surface of sediment is more chaotic, as for instance in a perched basin (OCNG8-12 to OCNG8-17). The surface of the sediment is much more perturbed on this eastern flank than on the western flank of profile 27, including apparent folding or faulting of sediments (Fig. 5). The origin of this deformation is not known, but perhaps it has led to more exposed basement rock, providing additional channels for fluids to enter and exit the volcanic crust.

Statistical analysis for each profile (Table 1) shows that heat flow decreases from North (profile 23) to south (profile 28), but conversely does not show a difference between the west and east flanks values.

5.2. Conductive versus low heat flow in typical ridge flank areas

The effects of hydrothermal circulation on the surface heat flow have been identified by Lister (1970, 1972) in the Juan de Fuca

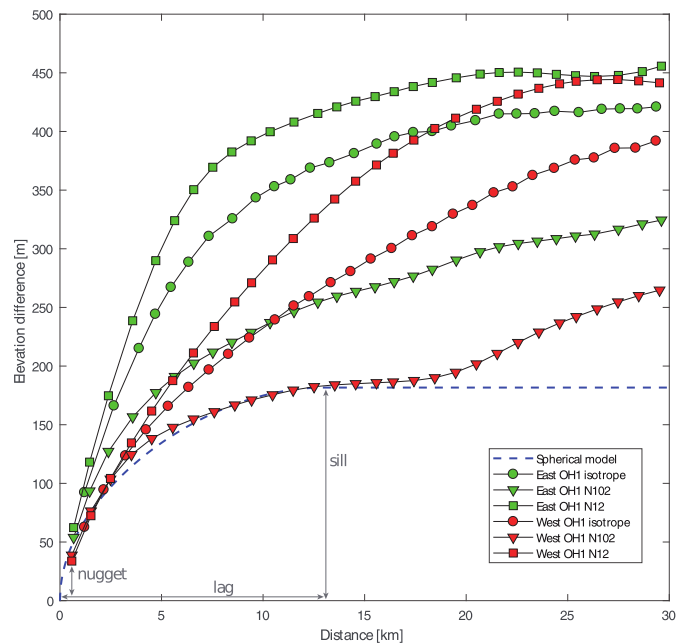


Fig. 6. Variograms of bathymetry in the study area. Variograms are calculated in different ways in order to outline the variation of relief with directions, on both flanks of the ridge: two directions are used (N102 and N12 along and perpendicular to the direction of accretion) as well as non-directional (isotropic) variogram. An example of a theoretical fit by a spherical variogram is shown for the case West OH1 N102: only the first part of the experimental variogram is used to determine the nugget effect, sill and lag values.

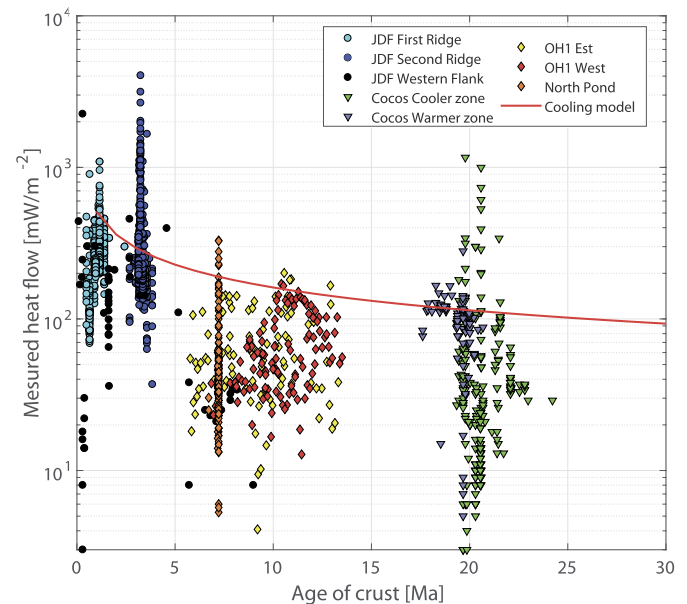


Fig. 7. Heat flow versus age of the sea-floor for several areas associated with hydrothermal circulation. Red line represents a conductive cooling model (Stein and Stein, 1992). (For interpretation of the references to color in this figure, the reader is referred to the web version of this article.)

area. Several high resolution studies were subsequently completed on the eastern flank of the Juan de Fuca ridge (Davis et al., 1989, 1992; Hutnak et al., 2006) and additional studies have been completed on the flanks of the East Pacific Rise and Cocos-Nazca Ridge (Villinger et al., 2002; Fisher et al., 2003b; Hutnak and Fisher, 2007; Fisher and Wheat, 2010). Heat flow as a function of age is shown in Fig. 7 for these previous studies and for the present work, and compared to a conductive cooling model (Stein and Stein, 1992). The eastern Juan de Fuca and the Dorado seamount

Table 1
Heat Flow and relief statistics for several off-axis areas. Heat Flow: avg. is arithmetic mean, σ standard deviation and q/q_0 fraction of the conductive value. Variogram: nug. is nugget effect (i.e. local relief). All variogram parameters were calculated with a spherical model. Resolution of topography is 30 sec of arc (≈ 1 km) except for seismic profiles (L23, L24...) for which a resolution of 500 m was used. For OH1, isotropic (isotr.) and directional (N12 and N102) are compared. For Juan de Fuca, Cocos plate and North Pond, only isotropic variograms were used.

Area			Heat flow					Seabottom variogram			Basement variogram										
			N	avg.	σ (mWm ⁻²)	median	q/q ₀	nug. (m)	lag (km)	sill (m)	nug. (m)	lag (km)	sill (m)								
OH1	West	isotr.	111	66	38	52	0.41	60	30	390	30	12	239								
		N102						40	13	180											
		N12	42	84	46	66	0.53	40	27	445	24	7	225								
		L23						10	12	90											
		L24						14	6	169											
		L25						3	62	18				55	0.40	15	6	102	25	7	110
		L26						11	71	34				59	0.45	15	9	107	35	7	187
		L27						32	53	23				51	0.36	12	12	113	28	11	219
L28	23	53	28	47	0.36	10	11	115	36	8	207										
OH1	East	isotr.	97	67	46	55	0.39	75	24	418	45	10	274								
		N102						55	15	265											
		N12	5	155	33	141	1.02	60	20	445	47	11	394								
		L23						33	10	200											
		L24						10	94	41				110	0.56	33	11	339	50	5	253
		L25						9	74	41				61	0.47	24	6	161	45	7	253
		L26						8	73	31				67	0.44	20	9	126	41	6	202
		L27						40	54	36				42	0.33	15	10	103	49	12	332
L28	22	52	36	54	0.29	13	12	187													
Juan de Fuca		HT-FR	474	268	126	261	0.54	20	15	71											
		SR	590	334	346	231	1.19	11	4	21											
		West	53	161	313	104	0.33	57	28	353											
Cocos plate		cool	217	68	135	32	0.60	28	15	122											
		warm	111	97	39	105	0.84	11	20	74											
North Pond			146	60	58	41	0.32	80	13	331											

(Cocos plate) areas show a wide distribution of heat flow values that range from well above to well below the prediction of the conductive model (Fig. 7). In these areas, high and low heat flow values can be related to local convection where there is basement relief below flat sediments, and the discharge and recharge parts of hydrothermal systems, in which seawater is channelized in the uppermost basaltic crust across a network of seamounts (Davis et al., 1989; Fisher et al., 2003a; Hutnak et al., 2006, 2008). Fisher et al. (2003a) have shown that these fluids can flow over distance as large as 50 km. In the Cocos area, high heat flow values are measured near the Dorado seamount (Fig. 7), considered a discharge zone for fluids, but most of measurements are low, and the average heat flow is 40 percent of the conductive value (Fisher et al., 2003b; Hutnak et al., 2008). The distance over which recharging fluids circulate to Dorado seamount is at least 20 km (Wheat and Fisher, 2008). Fisher and Wheat (2010) consider that the eastern Juan de Fuca and the Cocos ridge regions represent two distinct end-members of hydrothermal circulation on ridge flanks, (i) one with slow rates and long residence times, on 3.5–3.6 M.y. old seafloor on the eastern flank of Juan de Fuca Ridge, and (ii) one with high flow rates and short residence times in the Cocos ridge area. Lister (1972) explained the low heat flow values in western Juan de Fuca by the lack or thin cover of sediment. In the OH1 segment, the thickness of sediments in the off-axis basins (several hundreds of meters) is similar to that at the eastern Juan de Fuca and Cocos ridge area, but the morphology of these basins differs significantly: rather than isolated seamounts, basement highs form ridges that mostly trend parallel to the ridge leading to many areas of volcanic rock exposure and the possibility for large fluid flow in many directions. Heat flow pattern in OH1 is rather similar to the North Pond area in the central Atlantic, where values are systematically low and show a similar spatial increase (to the west for North Pond, to the north or the west for OH1). The distribution of heat flow values is also very similar for North Pond and OH1 (Fig. 7).

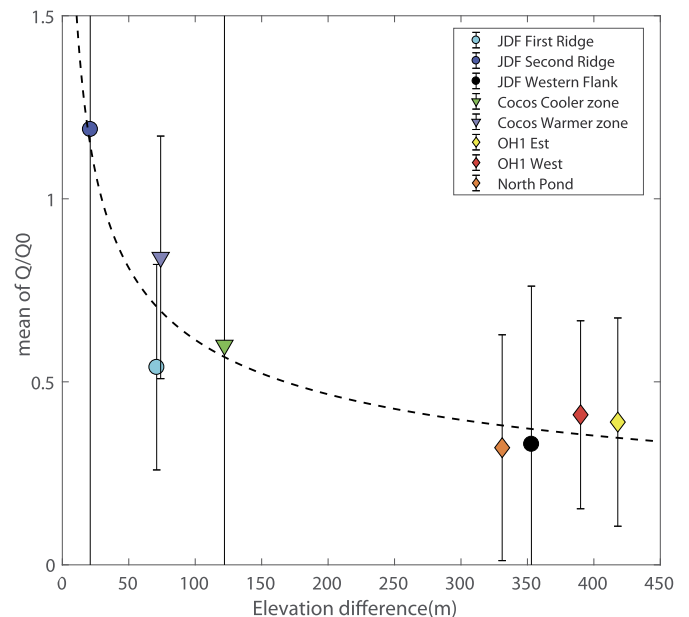


Fig. 8. Fraction of the conductive heat flow vs relief. Q is the average heat flow measured at a specific site and Q_0 is the conductive heat flow (estimated as a function of seafloor age). Relief is defined by the sill of variograms (see Fig. 6). Dash line is a speculative power law fit: $\frac{Q}{Q_0} = 3.8792S^{-0.4}$, where S is the sill of the variogram (m).

5.3. Heat flow and basement morphology in ridge flank areas

Hasterok et al. (2011) have considered the distance to seamounts and the sediment thickness as first order parameters controlling hydrothermal circulation in the off-axis oceanic crust. Var-

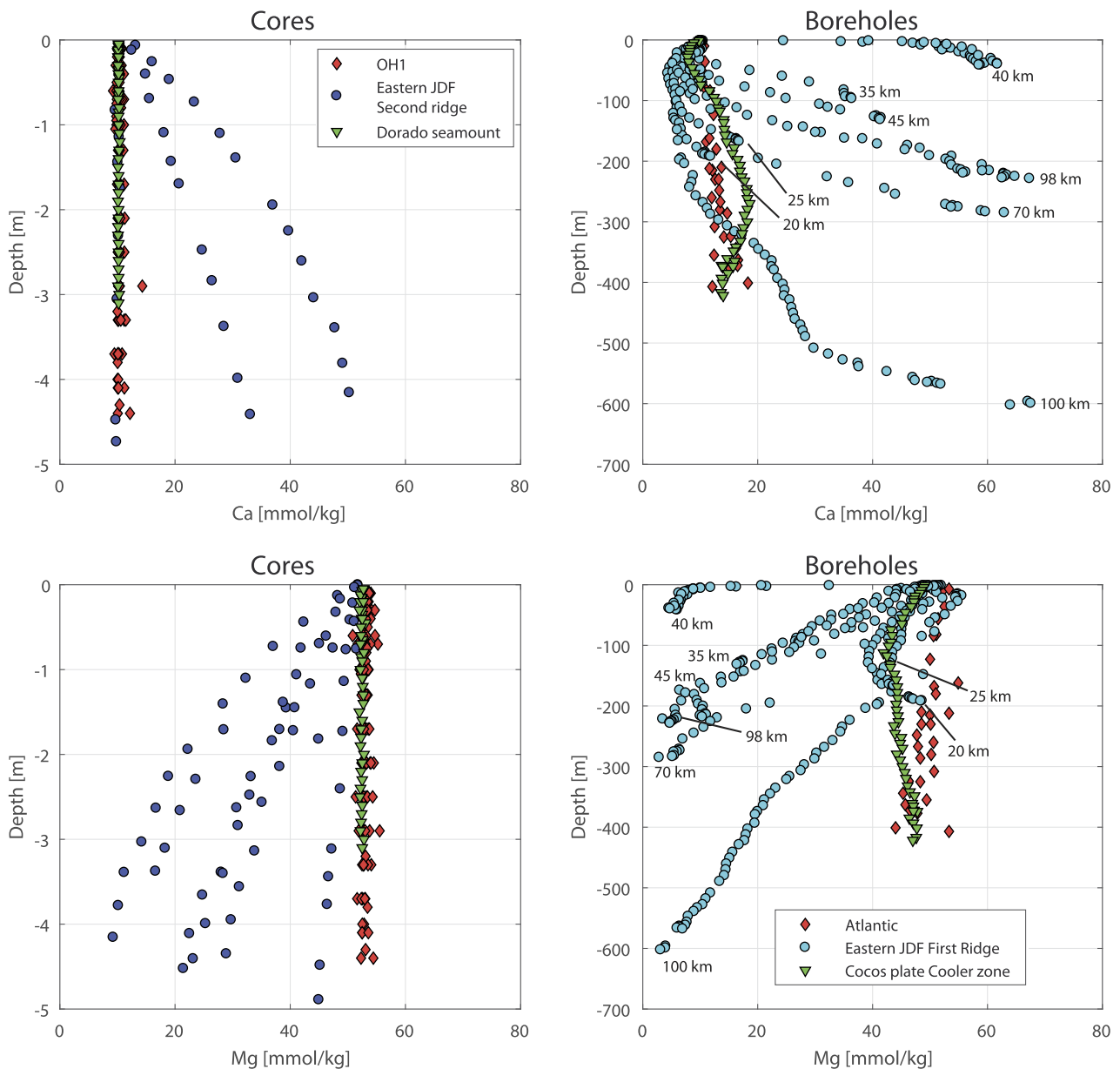


Fig. 9. Comparison of pore water concentrations for four areas associated with hydrothermal circulation. Upper panels show calcium concentrations and lower panel magnesium concentration. Left column represents cores data: Wheat and Mottl (1994); Wheat et al. (2000) for Juan de Fuca, Wheat and Fisher (2008); Fisher and Wheat (2010) for Cocos area and this study for Oceanograflu. Right column boreholes data: IODP Leg 168 (Elderfield et al., 1999) for Juan de Fuca, IODP Leg 170 (Kimura et al., 1997) for Cocos area and DSDP 82 (Drake et al., 1985) and DSDP 94 (Wilson and Miles, 1987) for the north Atlantic. For Juan de Fuca, the distance to the ridge is shown for each borehole.

igrams of the topography, which can describe seafloor roughness, may thus be a proxy for the efficiency of hydrothermal processes. Variograms of the seafloor topography were generated for OH1, North Pond, east and west flanks of Juan de Fuca and Cocos plate region with the GEBCO global elevation database (~1 km resolution). For OH1, directional variograms (along the spreading direction and parallel to the ridge axis) were also calculated. Variograms parameters were determined with a spherical model and are reported in Table 1. These parameters are systematically higher for OH1, west of the Juan de Fuca Ridge and North Pond than for east of Juan de Fuca and Cocos Plate. In addition, a statistical correlation exists between the fraction of conductive heat flow measured at the surface and the observed relief (Fig. 8). Although it needs further investigation, effect of hydrothermal circulation on surface heat flow apparently increases up to 60% for relief of 200 m and then stabilizes.

5.4. Fluid circulations and pore water composition

The circulation of fluids in the oceanic basement leads to a redistribution of heat, and to a redistribution of chemical species caused by alteration of basalts and overlying sediment. The amount exchanged during this alteration is linked to the temperature and to the residence time of water in the crust (Bischoff and Seyfried, 1978; Seyfried and Bischoff, 1979; Wheat and Mottl, 1994). Evidence for basalt alteration exists in the eastern Juan de Fuca area, where measured concentrations of major elements in pore waters in deep holes and in superficial cores are significantly different from that of seawater: for instance, calcium and magnesium are progressively enriched (or depleted) with depth (Fig. 9). This is caused by the alteration of basalt and the subsequent diffusion of calcium and magnesium in the sediment. Fig. 9 illustrates that the gradient of concentration increases with the distance to the

recharge zone, attesting to the existence of a critical distance (or a critical residence time) for changes in pore water composition. Empirical observations in eastern Juan de Fuca constrain this distance to about 40–50 km (Buatier et al., 1998; Mottl et al., 1998; Elderfield et al., 1999). The temperature of the fluids at the basement–sediment interface is also relatively high 60 °C (Davis et al., 1999) because of the young age of the crust and the thick sediment cover. By contrast, calcium and magnesium concentrations at Cocos and OH1 areas remain similar to seawater at all depths (Fig. 9). This is readily explained by basalt alteration being limited by the low temperature and short residence times.

DSDP hole 82 and 94 (Fig. 1) show constant concentrations of calcium and magnesium over the total thickness of the sedimentary basins (Fig. 9). Similar observations are made for the Cocos area where concentrations do not vary significantly in the basement (last point along borehole, ODP hole 1039). Rapid hydrothermal circulation in that area keeps basement fluids cool and relative unaltered. Observed or extrapolated temperatures at the basement–sediment interface are 20 °C for the Cocos area (Hutnak et al., 2008) and only 12 °C in Atlantic for 30 Ma old crust age (Hill and Cande, 1985). These temperatures also correspond to calculated values from previously cited conductive cooling models for the appropriate crustal age (Sclater and Francheteau, 1970; Davis and Lister, 1974; Stein and Stein, 1992). In addition, the residence time is probably too short (circulation path < 20 km for Cocos and less for OH1) for significant alteration and for heat conduction to significantly warm the water.

6. Conclusions

We present heat flow measurements and pore water compositions from the Oceanograflu survey, a marine geophysical study designed to identify hydrothermal circulation on a typical segment of the Mid-Atlantic Ridge (OH1). We compared the results to similar studies (North Pond in the northern Atlantic ocean, Juan de Fuca and central Cocos plate in the Pacific ocean). Heat flow from OH1 study is generally lower, but can reach or approach the conductive value in several locations where sediment is thicker, more continuous and where fewer basement outcrops exist. Pore fluids from sediments in this area are relatively homogeneous and similar in composition to seawater, consistent with large circulation of cool and unaltered hydrothermal fluids in the underlying volcanic rocks. The spatial variations of heat flow suggest that hydrothermal processes are strongly related to the observed relief, consistent with slow spreading ridge morphology. A large surface of exposed basement or sediment affected by faults provides short pathways for fluids, with little opportunity for them to equilibrate with temperatures of host rock and exchange significant amounts of chemical species. Hydrothermal efficiency, defined as the fraction of conductive heat flow measured at the sea bottom, and local relief in these different regions are strongly correlated and could define some empirical relationship to characterize the global magnitude of fluid circulation.

Acknowledgements

This contribution IGP n° 3879. The two reviews by Andy Fisher and an anonymous reviewers provided helpful criticisms and thoughtful suggestions that improved the manuscript. Editor Michael Bickle also provided helpful suggestions. This work benefited from discussions and reviews of early versions by Sylvie Leroy, Xavier Guichet and Brigitte Doligez. We thank captain Philippe Moimeaux and the crew of R/V “l’Atalante” for their technical assistance. The cruise and the geochemical analyses were supported by the French naval facilities and CNRS/INSU funds through program AO/SYSTER. We especially thank Olivier Crisp

(LOMIC Banyuls), Vasileios Mavromatis (GET Toulouse), Livio Ruffin (IFREMER Brest) and Claire Bassoulet (IUEM Brest) for their kind assistance. VLG PhD thesis was funded by IFPEN.

Appendix A. Supplementary material

Supplementary material related to this article can be found online at <https://doi.org/10.1016/j.epsl.2017.11.035>.

References

- Anderson, R.N., Langseth, M.G., Hobart, M.A., 1979. Geothermal convection through oceanic crust and sediments in the Indian Ocean. *Science* 204, 828–832. <http://www.jstor.org/stable/1748633>.
- Berner, R.A., 1971. *Principles of Chemical Sedimentology*. McGraw-Hill.
- Bischoff, J., Seyfried, W., 1978. Hydrothermal chemistry of seawater from 25 °C to 350 °C. *Am. J. Sci.* 278, 838–860.
- Bougault, H., Cande, S.C., et al., 1985. Site 560. In: DSDP Volume LXXXII. US Gov. Print. Off.
- Buatier, M.D., Monnin, C., Davis, E.E., Fisher, A.T., 1998. Circulation hydrothermale dans le flanc est de la ride de Juan de Fuca. *Résultats du leg ODP 168*. C. R. Acad. Sci., Sér. 2, Sci. Terre Planètes (Earth and Planetary Science) 326 (3), 201–206.
- Cannat, M., et al., 1999. Campagne sudaçores. N.O. L’Atalante, rapport de mission. Tech. rep. CNRS/Université Paris 6.
- Davis, E.E., Chapman, D.S., Forster, C.B., Villinger, H., 1989. Heat-flow variations correlated with buried basement topography on the Juan de Fuca Ridge. *Nature* 342, 533–537.
- Davis, E.E., Chapman, D.S., Wang, K.L., Villinger, H., Fisher, A.T., Robinson, S.W., Grigel, J., Pribnow, D.F.C., Stein, J.S., Becker, K., 1999. Regional heat flow variations across the sedimented Juan de Fuca Ridge eastern flank: constraints on lithospheric cooling and lateral hydrothermal heat transport. *J. Geophys. Res.* 104 (B8), 17675–17688.
- Davis, E.E., Chapman, N.R., Mottl, M.J., Bentkowski, W.J., Dadey, K., Forster, C.B., Harris, R.N., Nagihara, S., Rohr, K., Wheat, C.G., Whitticar, M., 1992. Flankflux: an experiment to study the nature of hydrothermal circulation in young oceanic crust. *Can. J. Earth Sci.* 29 (5), 925–952.
- Davis, E.E., Lister, C.R.B., 1974. Fundamentals of ridge crest topography. *Earth Planet. Sci. Lett.* 21, 405–413.
- Davis, E.E., Wang, K., He, J., Chapman, D.S., Villinger, H., Rosenberger, A., 1997. An unequivocal case for high Nusselt number hydrothermal convection in sediment buried igneous oceanic crust. *Earth Planet. Sci. Lett.* 146, 137–150.
- Detrick, R.S., Needham, H.D., Renard, V., 1995. Gravity anomalies and crustal thickness variations along the mid-Atlantic ridge between 33°N and 40°N. *J. Geophys. Res.* 100 (B3), 3767–3787.
- Drake, N., Rhodes, J., Autio, L., 1985. Geochemistry of basalts from deep sea drilling project holes 556–564. In: *Initial Reports of the Deep Sea Drilling Project*. U.S. Government Printing Office.
- Dunn, R.A., Lekić, V., Detrick, R.S., Toomey, D.R., 2005. Three-dimensional seismic structure of the mid-Atlantic ridge (35°N): evidence for focused melt supply and lower crustal dike injection. *J. Geophys. Res.* 110 (B9), B09101.
- Elderfield, H., Wheat, C.G., Mottl, M.J., Monnin, C., Spiro, B., 1999. Fluid and geochemical transport through oceanic crust: a transect across the eastern flank of the Juan de Fuca Ridge. *Earth Planet. Sci. Lett.* 172 (1–2), 151–165.
- Fisher, A.T., Davis, E.E., Hutnak, M., Spiess, F.N., Zuhlsdorff, L., Cherkaoui, A., Christiansen, L.B., Edwards, K., Macdonald, R., Villinger, H., Mottl, M.J., Wheat, C.G., Becker, K., 2003a. Hydrothermal recharge and discharge across 50 km guided by seamounts on a young ridge flank. *Nature* 421 (6923), 618–621.
- Fisher, A.T., Stein, C.S., Harris, R.N., Wang, K.L., Silver, E.A., Pfender, M., Hutnak, M., Cherkaoui, A., Bodzin, R., Villinger, H., 2003b. Abrupt thermal transition reveals hydrothermal boundary and role of seamounts within the Cocos plate. *Geophys. Res. Lett.* 30 (11), 1550, pp. 10.
- Fisher, A.T., Wheat, C.G., 2010. Seamounts as conduits for massive fluid, heat, and solute fluxes on ridge flanks. *Oceanography* 23.
- Hasterok, D., Chapman, D., Davis, E., 2011. Oceanic heat flow: implications for global heat loss. *Earth Planet. Sci. Lett.* 311 (3–4), 386–395.
- Hill, I., Cande, S., 1985. Thermal measurements and seawater downflow into 35 Ma old ocean crust, central North-Atlantic. In: *Initial Reports of the Deep Sea Drilling Project*, vol. 82, pp. 361–368.
- Hutnak, M., Fisher, A., Harris, R., Stein, C., Wang, K., Spinelli, G., Schindler, M., Villinger, H., Silver, E., 2008. Large heat and fluid flux driven through mid-plate outcrops on ocean crust. *Nat. Geosci.* 1, 611–614.
- Hutnak, M., Fisher, A., Stein, C., Harris, R., Wang, K., Silver, E., Spinelli, G., Pfender, M., Villinger, H., MacKnight, R., Costa Pisani, P., Deshon, H., Diamante, C., 2007. The thermal state of 18–24 Ma upper lithosphere subducting below the Nicoya Peninsula, northern Costa Rica margin. In: *MARGINS Theoretical Institute: SIEZE Volume*.
- Hutnak, M., Fisher, A.T., 2007. Influence of sedimentation, local and regional hydrothermal circulation, and thermal rebound on measurements of seafloor heat flux. *J. Geophys. Res.* 112, B12.

- Hutnak, M., Fisher, A.T., Zühlsdorff, L., Spiess, V., Stauffer, P.H., Gable, C.W., 2006. Hydrothermal recharge and discharge guided by basement outcrops on 0.7–3.6 Ma seafloor east of the Juan de Fuca ridge: observations and numerical models. *Geochem. Geophys. Geosyst.* 7 (7), Q07002.
- Kimura, G., Silver, E., Blum, P., et al. (Eds.), 1997. *Proceedings of the Ocean Drilling Program, 170 Initial Reports*. Ocean Drilling Program.
- Langseth, M.G., Becker, K., Von Herzen, R.P., Schultheiss, P., 1992. Heat and fluid flux through sediment on the western flank of the mid-Atlantic ridge: a hydrogeological study of North pond. *Geophys. Res. Lett.* 19 (5), 517–520.
- Langseth, M.G., Herman, B.M., 1981. Heat transfer in the oceanic crust of the Brazil basin. *J. Geophys. Res.* 86 (B11), 10805–10819.
- Langseth, M.G., Le Pichon, X., Ewing, M., 1966. Crustal structure of the mid-ocean ridges, 5, heat flow through the Atlantic Ocean floor and convection currents. *J. Geophys. Res.* 71, 5321–5355.
- Lister, C.R.B., 1970. Heat flow west of the Juan de Fuca Ridge. *J. Geophys. Res.* 75, 2648–2654.
- Lister, C.R.B., 1972. On the thermal balance of a mid-ocean ridge. *Geophys. J. R. Astron. Soc.* 26, 515–535.
- Lucazeau, F., Bonneville, A., Escartín, J., Von Herzen, R.P., Gouze, P., Carton, H., Cannat, M., Vidal, V., Adam, C., 2006. Heat-flow variations on a slowly accreting ridge: constraints on the hydrothermal and conductive cooling for the lucky strike segment (mid Atlantic ridge, 37°N). *Geochem. Geophys. Geosyst.* 7 (7), Q07011.
- Mathéron, G., Krumbein, W.C., 1970. Structures aléatoires et géologie mathématique. *Rev. Inst. Int. Stat. (Review of the International Statistical Institute)* 38 (1), 1.
- Millero, F.J., Graham, T.B., Huang, F., Bustos-Serrano, H., Pierrot, D., 2006. Dissociation constants of carbonic acid in seawater as a function of salinity and temperature. *Mar. Chem.* 100 (1–2), 80–94.
- Mottl, M.J., Wheat, G., Baker, E., Becker, N., Davis, E., Feely, R., Grehan, A., Kadko, D., Lilley, M., Massoth, G., Moyer, C., Sansone, F., 1998. Warm springs discovered on 3.5 Ma oceanic crust, eastern flank of the Juan de Fuca Ridge. *Geology* 26 (1), 51–54.
- Rabain, A., Cannat, M., Escartín, J., Pouliquen, G., Deplus, C., Rommevaux-Jestin, C., 2001. Focused volcanism and growth of a slow spreading segment (mid-Atlantic Ridge, 35°N). *Earth Planet. Sci. Lett.* 185, 211–224.
- Roko, R., Daemen, J., Myers, D., 1997. Variogram characterization of joint surface morphology and asperity deformation during shearing. *Int. J. Rock Mech. Min. Sci.* 34 (1), 71–84.
- Schmidt-Schierhorn, F., Kaul, N., Stephan, S., Villinger, H., 2012. Geophysical site survey results from North pond (Mid-Atlantic Ridge). In: Edwards, K.J., Bach, W., Klaus, A., et al. (Eds.), *Proceedings IODP, vol. 336. Integrated Ocean Drilling Program Management International, Inc.*
- Slater, J.G., Francheteau, J., 1970. The implication of terrestrial heat flow observations on current tectonic and geochemical models of the crust and upper mantle of the Earth. *Geophys. J. R. Astron. Soc.* 20, 509–542.
- Seeberg-Elverfeldt, J., Schlüter, M., Feseker, T., Kölling, M., 2005. Rhizon sampling of porewaters near the sediment–water interface of aquatic systems. *Limnol. Oceanogr., Methods* 3 (8), 361–371.
- Seyfried, W., Bischoff, J., 1979. Low temperature basalt alteration by sea water: an experimental study at 70 °C and 150 °C. *Geochim. Cosmochim. Acta* 43 (12), 1937–1947.
- Seyfried, W.E., Mottl, M.J., 1982. Hydrothermal alteration of basalt by seawater under seawater-dominated conditions. *Geochim. Cosmochim. Acta* 46 (6), 985–1002.
- Staudigel, H., Hart, S.R., Richardson, S.H., 1981. Alteration of the oceanic crust: processes and timing. *Earth Planet. Sci. Lett.* 52 (2), 311–327.
- Stein, C.S., Stein, S., 1992. A model for the global variation in oceanic depth and heat flow with lithospheric age. *Nature* 359, 123–129.
- Stein, C.S., Stein, S., 1994. Constraints on hydrothermal heat flux through the oceanic lithosphere from global heat flow. *J. Geophys. Res.* 99 (B2), 3081–3096.
- Villinger, H., Grevemeyer, I., Kaul, N., Hauschild, J., Pfender, M., 2002. Hydrothermal heat flux through aged oceanic crust: where does the heat escape? *Earth Planet. Sci. Lett.* 202 (1), 159–170.
- Von Herzen, R.P., Cordery, M.J., Detrick, R.S., Fang, C., 1989. Heat flow and the thermal origin of hotspot swells: the Hawaiian swell revisited. *J. Geophys. Res.* 94, 13–783.
- Wheat, C.G., Elderfield, H., Mottl, M.J., Monnin, C., 2000. Chemical composition of basement fluids within an oceanic ridge flank: implications for along-strike and across-strike hydrothermal circulation. *J. Geophys. Res.* 105, 13437–13447.
- Wheat, C.G., Fisher, A.T., 2008. Massive, low-temperature hydrothermal flow from a basaltic outcrop on 23 Ma seafloor of the Cocos Plate: chemical constraints and implications. *Geochem. Geophys. Geosyst.* 9 (12), Q12014.
- Wheat, C.G., Mottl, M.J., 1994. Hydrothermal circulation, Juan de Fuca Ridge eastern flank: factors controlling basement water composition. *J. Geophys. Res.* 99, 3067–3080.
- Wheat, C.G., Mottl, M.J., Fisher, A.T., Kadko, D., Davis, E.E., Baker, E.T., 2004. Heat flow through a basaltic outcrop on a sedimented young ridge flank. *Geochem. Geophys. Geosyst.* 5 (12), Q12006.
- Wilson, T., Miles, D., 1987. On the utility of chemical data for the detection of vertical pore-water movement in marine sediments. In: *Initial Reports of the Deep Sea Drilling Project*. U.S. Government Printing Office.